Trajectory planning issues in cuspidal commercial robots

Durgesh Haribhau Salunkhe, Damien Chablat, Philippe Wenger

Trajectory planning issues in cuspidal commercial robots

Durgesh Haribhau Salunkhe[1], Damien Chablat[1] and Philippe Wenger[1]

***Abstract*— A cuspidal serial robot can travel from one inverse kinematic solution to another without crossing a singularity. Cuspidal robots ask for extra care and caution in trajectory planning, as identifying an *aspect* related to one unique inverse kinematic solution is not possible. The issues related to motion planning with cuspidal robots are related to the inherent property arising from the geometric design of the robot. The cuspidality property has not been considered in recent industrial 6R robots with a non-spherical wrist. In this work, cuspidality is illustrated with the JACO robot (gen 2, non-spherical wrist), a serial arm by Kinova Robotics which is deployed in various applications and is cuspidal in nature. A nonsingular change of solutions for the robot is provided to highlight the effect of cuspidal robots on the interference with the environment. The pose with multiple inverse kinematic solutions in an aspect is presented. Problems in choosing the initial solution of the path in cuspidal robots, and its consequence, is illustrated with an example path in the workspace of the JACO robot. The paper presents the importance of cuspidality analysis of 6R robots and the implications of neglecting it.**

I. INTRODUCTION

Wrist-partitioned anthropomorphic serial robots have been conventional designs for 6R commercial robots. The inverse kinematics and the singularities of such robots can be easily determined. Since the determinant of the Jacobian matrix, **J**, factors into three components, the singularity-free connected regions in the joint space, named *aspects*, can be determined and visualized. From the analysis of these robots, it was assumed that every inverse kinematic solution of a serial robot lies in an aspect. This was proved to be incorrect, and counterexamples were presented in 1988 by Parenti-Castelli [1] in two 6R robots and by Burdick in 1989 [2] in 3R robots. *Cuspidal* robots are serial manipulators that can travel from one inverse kinematic solution (IKS) to another without crossing a singularity. The ability to follow a path effecting the change of inverse kinematic solutions without crossing a singularity is termed as cuspidality and the path is called a *nonsingular change of solutions*. The name '*cuspidal*' originated from the existence of a cusp in the singularity locus in the workspace of cuspidal 3R robots [3]. Cuspidality exists in both serial and parallel manipulators [4], [5], but this paper focuses on serial manipulators only. Most commercial robots implemented in the past are non-cuspidal and the posture in which a non-cuspidal robot is operating can be easily identified with the signs of the factors of the determinant of **J** [6]. Instead, posture identification is not possible in cuspidal robots as the determinant does not usually factor and there are multiple solutions in one aspect [7]. Cuspidal robots were first formalized in [7] and later extensively studied in [8]–[12]. Different approaches were implemented to identify and classify 3R *orthogonal* robots (i.e. robots with three mutually orthogonal joint axes), based on cuspidality. Recently, it was proved that the existence of a cusp point is a necessary and sufficient condition for generic 3R robots to be cuspidal [13]. A certified algorithm to decide the cuspidality of non-redundant revolute-jointed robots was presented [14], allowing a designer to verify his designs for cuspidality. The cuspidality analysis of 3R robots can be extended to wrist-partitioned 6R robots. This is attributed to the reason that the singularities in the position and the orientation for such robots are decoupled. While 3R cuspidal robots have been extensively studied, the cuspidality study of 6R robots with non-spherical wrist is still ongoing, while more and more such robots appear on the market [15].

The issues related to path following in cuspidal robots are not only related to the algorithms used for trajectory planning, but also due to the inherent property arising from the geometric design of the manipulator. As designers move away from the conventionally implemented wrist-partitioned anthropomorphic architecture, there is a high chance that such robots have completely different kinematic properties. The cuspidality property seems to have been slipped from the consideration of the current designers around the world [15]. Recently, several industrial 6R robots with a non-spherical wrist have appeared. To the best of our knowledge, the only 6R robots with a non-spherical wrist that have been analyzed for the cuspidal property, are the UR-series robots from Universal Robots. Computer algebraic tools were used to show that these robots have eight aspects with no more than one IKS per aspect [16], leading to a conclusion that such robots are non-cuspidal. This is because UR robots have three parallel joint axes, a geometric simplification that was identified by Pieper as a solvability criterion [17]. In the absence of 3 parallel joint axes, 6R robots with a non-spherical wrist are likely to be cuspidal.

In this work, cuspidality is illustrated with the JACO robot (gen 2, non-spherical wrist) from Kinova robotics, which is used in various applications. The JACO robot was mainly designed for rehabilitation [18] and thus is employed near persons with disability and interacts with them in a few cases. Multiple IKS that belong to the same aspect are presented, and the implication of cuspidality on path planning is highlighted. The dangers of neglecting the cuspidality are detailed and the rationale behind limiting their use in collaborative environments is motivated too.

[1]Nantes Université, École Centrale Nantes, CNRS, LS2N, UMR 6004, 44000 Nantes, France {durgesh.salunkhe, damien.chablat, philippe.wenger}@ls2n.fr

II. PRELIMINARIES

In this section, few definitions are presented for a complete understanding of the cuspidal robots. Joint limits and obstacles are not considered in the current study.

A. Recall of important definitions

Aspects: The aspects are the largest singularity-free connected regions in the joint space of a robot [6].

Cuspidal robot: A cuspidal robot is a robot for which there exists a path in the joint space connecting two IKS without crossing the locus of critical points (i.e., meeting a singularity) in the joint space [19].

Nonsingular change of solutions: A nonsingular change of solutions is a connected path between two IKS which does not cross the locus of critical points in the joint space. In the workspace, a nonsingular change of solutions forms a closed loop. Indeed, the robot trajectory ends up at the same pose it started from, but in a different joint configuration. The singularities of generic 6R robots depend on $\theta_i, i = 2,..5$, and thus lie in a 4-dimensional space that cannot be visualized. It can be confirmed that a given change of solutions path is nonsingular if the determinant of the Jacobian matrix does not change sign along the path. Fig. 1 shows an example of a nonsingular change of solutions in a 3R robot. It can be seen that the path in the joint space never crosses the locus of critical points (shown in blue lines) and, accordingly, the determinant value does not change signs throughout the path.

B. Path repeatability of cuspidal robots

If a non-cuspidal robots is able to follow a prescribed closed path once, it can repeat the path in same direction multiple times. This is not always the case in cuspidal robots, where path repeatability depends on the initial IKS. This is well established for *3R robots*: a closed path corresponding to a nonsingular change of solutions can be followed only once in the same direction, no matter which initial IKS is chosen [10]. For 6R robots, the situation is even more delicate. It was reported in [1] that some 6R robots can repeat a closed path corresponding to a nonsingular change of solutions, while others cannot. This property of 6R robots to repeat or not a nonsingular change of solutions path has further implications in trajectory planning. If the pose of the end-effector can be changed with manual intervention and the trajectory is not pre-planned, it is not possible to identify the initial choice of IKS. Due to this reason, the use of 6R cuspidal robots in an interactive environment may not be suitable as it can lead to interference between the robot and its environment.

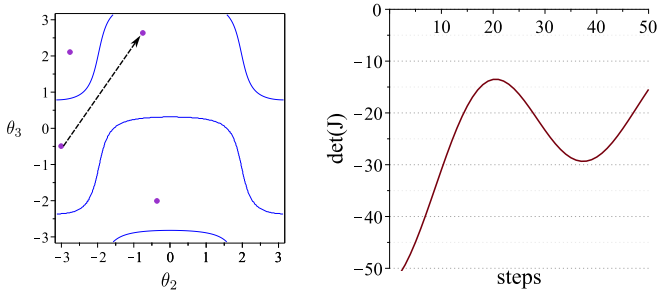

Fig. 1: Example of nonsingular change of solutions in the joint space and the progress of determinant value on the path Robot parameters: **d** = [0, 1, 0], **a** = [1, 2, $\frac{3}{2}$], α = [-$\frac{\pi}{2}$, $\frac{\pi}{2}$, 0], path = (-3, -0.5) to (-0.742, 2.628).

III. KINEMATIC ANALYSIS

In this section, the kinematic analysis of the JACO robot is presented. The methodology implemented to get the IKS is briefly revisited, and instances of end-effector pose with varying IKS are provided.

A. Inverse Kinematics

Table I shows the DH parameter table for the JACO robot. Here, d_i denotes the distance along the axis of i^{th} motor, a_i is the offset between i^{th} and $(i+1)^{th}$ frame and α_i is the orientation of $(i+1)^{th}$ the axis with respect to the i^{th} axis. The parameter d_6 does not affect the inverse kinematic solution and thus can be kept as a variable. For the purpose of this paper, d_6 = 160 mm. The JACO robot has an offset in the wrist, and thus a direct decoupled analysis cannot be implemented. Inverse kinematics for such robots with an offset in the wrist can be obtained by previously established algorithms for generic 6R robot [20], [21] or with methods applicable specifically to offset in the wrist [22], [23]. In this paper, the results are presented by using the methodology detailed in [23] as it is specific to the JACO design and is easy to implement. Using this method, a 16-degree-polynomial in $\tan\frac{\theta_1}{2}$ is obtained by eliminating the other joint variables. This polynomial with rational parameters is solved with the *Isolate* function [24] in *RootFinding* library available in Maple 2020. Then, straightforward backpropagation is used to obtain the rest of the joint variables.

B. Number of IKS in the JACO robot

It is a well-known result that a wrist-partitioned 6R robot has at most eight solutions. This is attributed to the decoupling between the positions and orientation of the end-effector and thus can be solved independently. The first 3R chain forms a regional manipulator and its inverse kinematics can be solved with a four degree inverse kinematics polynomial or two quadratics in cascade. The wrist provides two solutions for each orientation and thus, yields maximum of eight (4 × 2) solutions for a wrist-partitioned 6R robot. This does not hold true for robots with an offset in the wrist such

TABLE I: The DH parameters of the JACO robot

i	d_i (mm)	a_i (mm)	α_i (rad)	θ_i (rad)
1	275.5	0	$\pi/2$	θ_1
2	0	410	0	θ_2
3	13.3	207.3	$-\pi/2$	θ_3
4	103.8	0	$\pi/2$	θ_4
5	0	103.8	$-\pi/2$	θ_5
6	d_6	0	0	θ_6

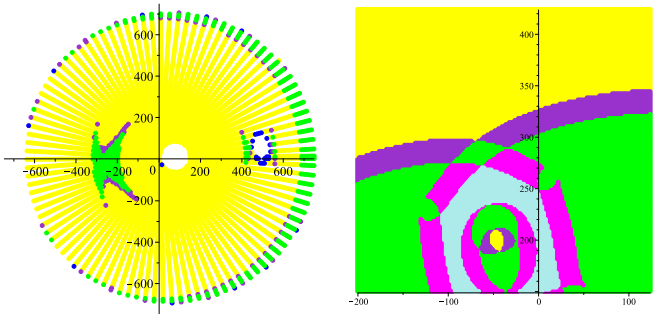

(a) Slice 1 (b) Zoomed section of Slice 2

Fig. 2: Regions with different number of IKS in 2D slice (xy-plane) in the workspace of JACO. The fixed orientation as a quaternion ($\mathbf{h}$) and fixed z-coordinate(mm) for the slices: Slice 1: $\mathbf{h}$ = 0.2565 + 0.033$\hat{\mathbf{i}}$ + 0.812$\hat{\mathbf{j}}$ + 0.582$\hat{\mathbf{k}}$, z = 560.56 Slice 2: $\mathbf{h}$ = 0.984 + 0.004$\hat{\mathbf{i}}$ + 0.103$\hat{\mathbf{j}}$ + 0.147$\hat{\mathbf{k}}$, z = 257.94

as the JACO robot. A case of end-effector pose with twelve IKS was exhibited in [23]. While, in the absence of joint limits and collisions, a pose in a nonsingular configuration of a wrist-partitioned 6R robot has either eight IKS or four IKS, it is shown that the Jaco robot can have two, four, six, eight, ten, or twelve IKS. It can be concluded from this finding that the workspace of the JACO robot is divided in multiple regions of varying number of IKS and thus the trajectory planning for such a robot is a non-trivial problem. This is because a desired path can cross singularities in the workspace and switch between multiple connected regions in the workspace with varying number of IKS. Figure 2 shows two different 2D slices in the workspace of the JACO robot with a fixed orientation and z-coordinate. The blue, yellow, dark orchid, green, magenta, and turquoise colors represent the end-effector pose with two, four, six, eight, ten, and twelve solutions, respectively. The slice in fig. 2a has regions with two, four, six, and eight solutions. It is worth noting that two voids appear in this slice. This is unusual in Puma-type robots. The slice in fig. 2b has four, six, eight, ten, and twelve solution regions.

IV. Cuspidality analysis

In this section, it is shown that the JACO robot is cuspidal and a path corresponding to nonsingular change of solutions is presented. The twelve solutions are equally distributed in two aspects, and an IKS from one aspect can be connected to other five present in the same aspect.

A. Investigating connectivity

The solutions for a particular pose of the end-effector is given in table II along with the sign of the determinant of the Jacobian matrix, det($\mathbf{J}$), at the corresponding joint configuration. To search for a nonsingular change of solutions, a linear interpolation between two IKS with the same determinant value was evaluated. If the determinant value changed sign along the linear interpolation, then the path was divided in three parts and the two non-extreme points of the path were recalculated by using the Nelder-Mead approach [25], to find the possible nonsingular change of solutions. This is a working algorithm to determine cuspidality of any robot and is faster to implement when compared to a more robust certified algorithm in [14]. The advantage of using Nelder-Mead approach to determine the connectivity of the given IKS is that the method is versatile and can adapt to constraints easily. This implies that the working algorithm can be extended to find a nonsingular change of solutions with joint limits and collision constraints of the robot too. Figure 3 & 4 show the progress of det($\mathbf{J}$) along the joint paths obtained from the algorithm. It is apparent that there are six solutions in aspect det($\mathbf{J}$) > 0 and six solutions in aspect det($\mathbf{J}$) < 0.

B. Nonsingular change of solutions

The visualization of a nonsingular change of solutions is presented in this subsection to emphasize the impact of the choice of initial IKS on the robot's interaction with the environment. Figure 5 shows the end-effector path corresponding to the nonsingularchange of solution from VII to VIII (Fig. 4a). The end-effector path is a closed loop. The nonsingular change of solutions in 3R robots is well understood and can be anticipated [10]. Indeed, the nonsingular change of solutions takes place strictly after crossing the locus of critical values (a workspace boundary associated to a singularity) and thus the trajectory passes through regions with different number of IKS [13]. This behavior has not been proved in 6R robots, and thus it is unclear whether a nonsingular change of solutions implies a path that passes through different connected regions in the workspace. It is straightforward to conclude from fig. 5 that the kinematic properties along the desired path are a direct result of the choice of initial IKS.

V. Issues in trajectory planning

In this section, the challenges in planning a trajectory with a cuspidal robot are highlighted by using JACO robot. As shown in fig. 2, it is known that there are multiple connected regions with varying numbers of IKS. It is well

TABLE II: Example enumeration of 12 IKS of a pose of the JACO robot.
Orientation: $\mathbf{h}$ = 0.549 + 0.497$\hat{\mathbf{i}}$ + 0.423$\hat{\mathbf{j}}$ + 0.522$\hat{\mathbf{k}}$, position(x,y,z)(mm) = (140.49, 47.13, 324.876)

IKS (sign(det))	θ_1 (rad)	θ_2 (rad)	θ_3 (rad)	θ_4 (rad)	θ_5 (rad)	θ_6 (rad)
I (+)	3.0675	1.0545	1.3090	2.4283	-1.2305	-2.3002
II (+)	2.4335	0.0936	1.5741	1.4311	2.3452	0.5391
III (+)	-0.8579	3.0408	1.5721	-1.5912	2.1625	0.5390
IV (+)	2.9132	0.2824	1.9297	-2.1648	-2.9685	-2.7165
V (+)	-0.2812	2.0346	1.8631	-0.5833	-1.0917	-2.4130
VI (+)	-0.2456	2.8156	1.3090	0.4882	-2.8301	-2.3003
VII (-)	-3.1201	0.7082	1.4904	2.62	-1.9637	-1.8817
VIII (-)	2.4730	0.0943	2.0281	-1.4916	-2.4244	2.4362
IX (-)	-0.1583	2.7025	1.4699	-0.0656	-2.5402	-1.9078
X (-)	-0.7501	1.9399	2.0268	-1.4270	0.6212	2.6291
XI (-)	-0.8046	3.0466	1.1135	1.5103	-2.2697	2.4394
XII (-)	2.5338	1.2022	1.1149	1.5839	0.6030	2.6322

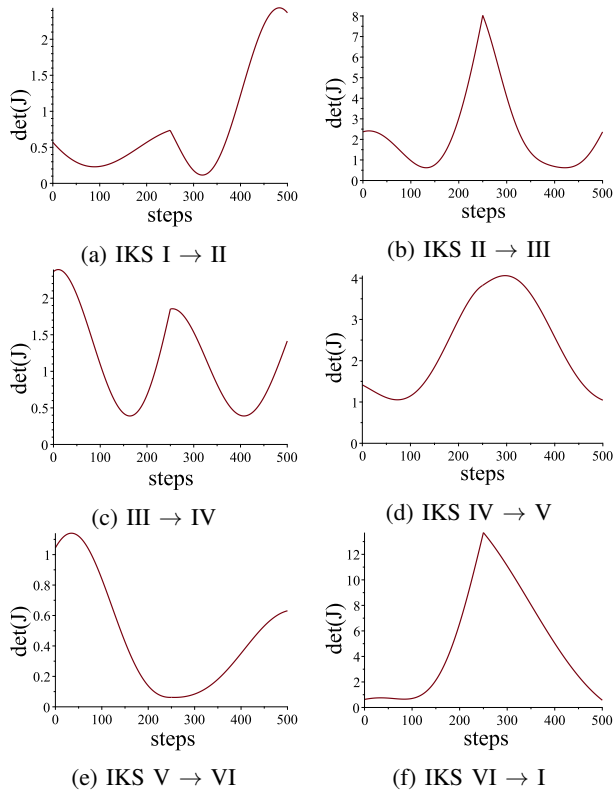

(a) IKS I → II (b) IKS II → III (c) III → IV (d) IKS IV → V (e) IKS V → VI (f) IKS VI → I

Fig. 3: Progress of the det(**J**) for six nonsingular change of solutions in aspect with positive determinant value

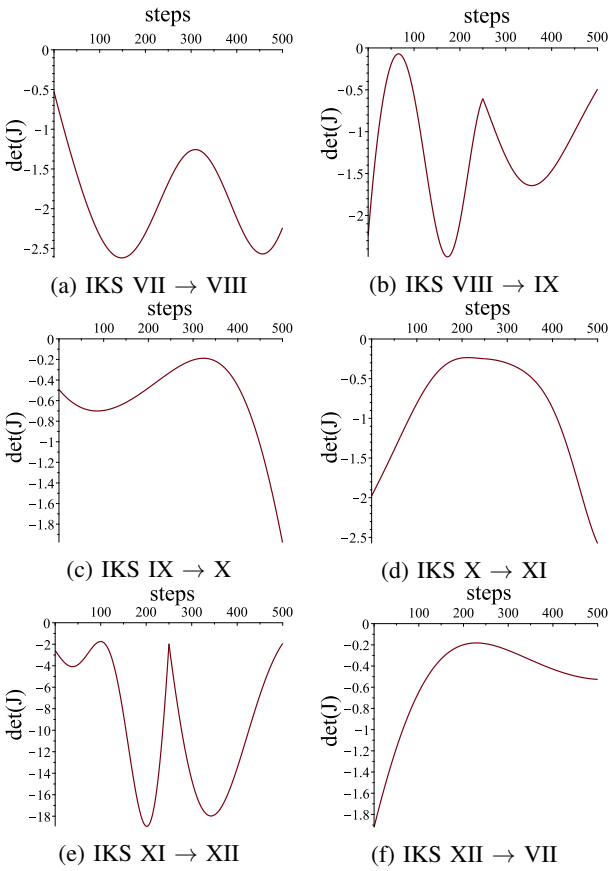

(a) IKS VII → VIII (b) IKS VIII → IX (c) IKS IX → X (d) IKS X → XI (e) IKS XI → XII (f) IKS XII → VII

Fig. 4: Progress of det(**J**) for six nonsingular change of solutions in aspect with negative determinant value

established that when a workspace boundary associated with a singularity is crossed, at least two solutions disappear (resp. appear) if the robot move toward a region with less IKS (resp. with more IKS) [26]. In classical path planning algorithms, a change of solution only occurs when det(**J**) changes sign. Thus, an end-effector path can be declared infeasible if det(**J**) changes sign. In the case of cuspidal robots, a jump to another IKS in the same aspect can be experienced without being detected, and this jump results into going off the planned end-effector path. Such a behavior has been recorded in the MICO robot earlier but lacks a detailed explanation of the error [15]. It is surprising to note that the issue in path planning of the JACO Gen 2 robot has not been widely reported. The authors' best guess is that either most of the planning done using this robot is in the joint space or the solutions are just declared infeasible if a critical value is encountered. The issues in planning were discussed with the company that manufactures the robot.

A. Issue 1: Choice of initial IKS

In order to better explain the issue of choosing a suitable initial IKS, the case of a 3R robot is presented in detail. The workspace and singularities of 3R robots have been extensively presented in [10], [13], and are revisited briefly in this paper. Figure 6 shows the singularities in both the joint space and the workspace of an example of a 3R orthogonal robot with DH-parameters similar to the one mentioned in fig. 1. Figure 6b illustrates a closed loop path that starts from a pose with four IKS and passes through two connected regions in the workspace. The level set representation [27] of a cross section of the workspace in $(\rho, z, \cos\theta_2)$ corresponding to the two aspects are shown in fig. 7b & 8b respectively. The dotted line represents the pose of the end-effector and the intersection of this line with the level set representation corresponds to one IKS. $\mathbf{q}_i$ is the IKS in the joint space of the robot and the corresponding point on the level set representation is given as $\mathbf{p}_i$. Depending upon the initial IKS, $\mathbf{q}_i$, the path is either feasible or infeasible. It can be deduced from fig. 1, fig. 7 and fig. 8 that if the trajectory starts from initial IKS $\mathbf{q}_2$ or $\mathbf{q}_3$, the closed loop path is infeasible. The path is feasible only if the initial IKS is either $\mathbf{q}_1$ or $\mathbf{q}_4$. Closed-loop paths that do not result in a change of IKS can be repeated but this is clearly not the case of nonsingular solution changing paths. This dependency of path feasibility and repeatability on the initial IKS pose several challenges in planning trajectories of 6R cuspidal robots. Being aware of the cuspidal property of a robot, the choice of initial IKS may not be a problem if the complete trajectory to be followed and the repeatability condition for the path are known prior to execution. Thus, it is of great importance that such robots are strictly used in environments with pre-planned trajectories. If deployed in collaborative areas (as is the present case for the Jaco robot), such robots are bound to error and can lead

(a) Initial solution (b) Intermediate path

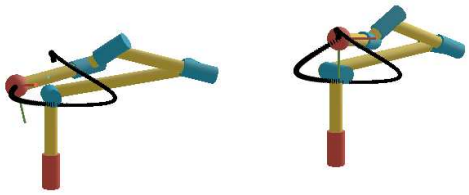

(c) Intermediate path (d) Final solution

Fig. 5: Nonsingular change of solutions: IKS VII $\rightarrow$ VIII.

to unexpected behavior and unforeseen scenarios.

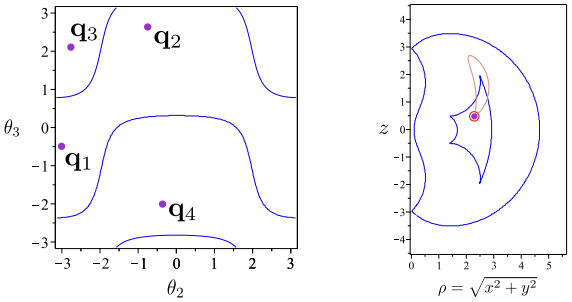

(a) Singularities in joint space (b) Singularities in workspace

Fig. 6: Singularities (blue lines) in the joint space and the workspace of a 3R orthogonal robot.

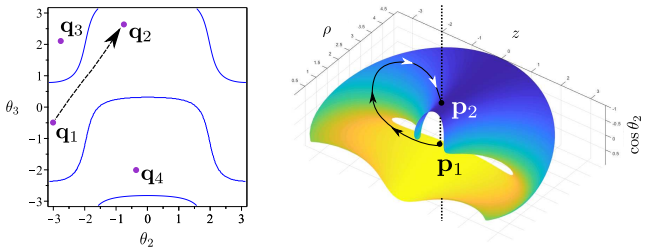

(a) Closed path starting from IKS $\mathbf{q}_1$ (b) Closed path as seen in the level set representation of one aspect

Fig. 7: An example of nonsingular change of solutions

B. Issue 2 : Repeatable and non-repeatable trajectories

In 3R robots, the transition between regions with 0, 2 and 4 IKS allows one to visualize the level set representation

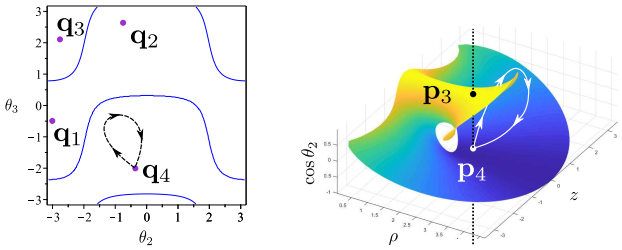

(a) Closed path starting from IKS $\mathbf{q}_4$ (b) Closed path as seen in the level set representation of another aspect

Fig. 8: Same path as in fig. 7 but without changing solutions

making the analysis easier than for 6R robots. For the JACO robot, there exists multiple accessibility regions with 6 possible number of IKS. This leads to many complicated possibilities and the planned path may include sudden jumps in the joint values. This sudden jump cannot be avoided by use of a generic planner that is unaware of the cuspidal property of the robot. An example trajectory is shown in fig. 9 which crosses regions with 4, 6 and 8 IKS. The trajectory is in the Slice 1 (refer to fig. 2a) and starts from point $\mathbf{a}(-180,0)$ and passes through point $\mathbf{b}(-180,200)$, $\mathbf{c}(-120,200)$ and $\mathbf{d}(-120,0)$ and returns to $\mathbf{a}$. Figures 10 and 11 show the time histories of the joint angles along the path. The dotted lines divide the path into four parts and represent the instances when the path crosses a region with a given number of IKS in the workspace. They are labeled as $(i \rightarrow j)$ denoting the change from a region with i solutions to the region with j solutions. The first and the fourth regions correspond to the path in a eight-solution region while the second and third regions correspond to the path in six- and four-solution regions, respectively. The blue color paths in each plot are the solutions in an aspect with $\det(\mathbf{J}) > 0$ while the red paths correspond to $\det(\mathbf{J}) < 0$. In fig. 10, $T_i, i = 1..8$ is a trajectory corresponding to each initial IKS. It can be seen that if the robot starts the path from IKS corresponding to T_3, T_4, T_7 or T_8, it soon meets a singularity. If the cuspidality of the robot is not taken into account, a sudden jump will take place to a solution available in the same aspect at the next discrete instance. For example, if the path is initiated from T_4 (resp. from T_3), after the first dotted line, $(8 \rightarrow 6)$, there will be a sudden jump to T_1, T_5 or T_8 (resp. to T_2, T_6 or T_7). In case of trajectory T_7 and T_8, there will be a sudden jump after $(6 \rightarrow 4)$ to T_2 or T_6 and T_1 or T_5, respectively. Some of these jumps are shown by green color lines in fig. 10. It is apparent that T_3, T_4, T_7 and T_8 are infeasible. Trajectories T_1 and T_5 whose initial IKS belongs to an aspect with $\det(\mathbf{J}) < 0$ necessarily correspond to a nonsingular change of solutions that are non-repeatable. The trajectory T_1 (resp. T_5) leads to change the IKS to the initial IKS of T_8 (resp. T_4). Trajectories T_2 and T_6 whose initial IKS belongs to an aspect with $\det(\mathbf{J}) > 0$ are the only two trajectories out of the eight possibilities that are repeatable and do not correspond to a nonsingular change of solutions.

Trajectories that pass through multiple regions with higher

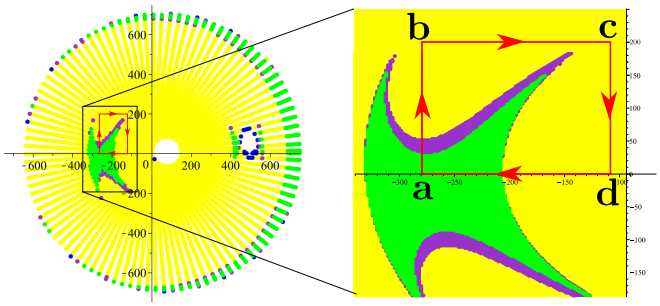

Fig. 9: A closed trajectory crossing multiple connected regions in the workspace of JACO robot

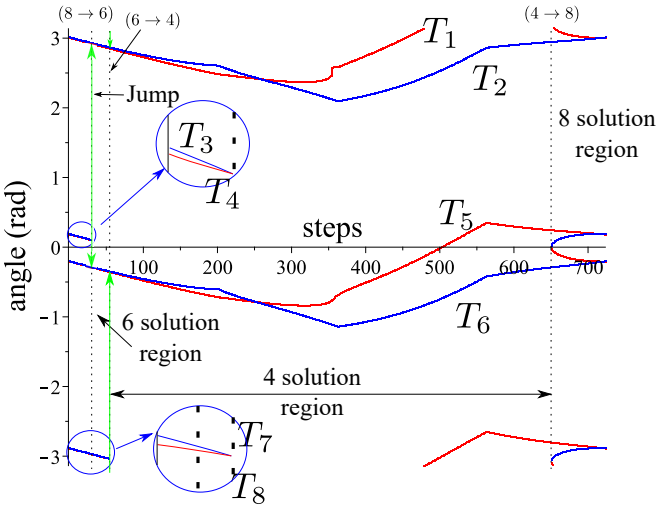

Fig. 10: Value of θ_1 along the closed path in fig. 9, with regions of 4, 6 and 8 IKS. Blue and red paths correspond to solutions in an aspect with $\det(\mathbf{J}) > 0$ and $\det(\mathbf{J}) < 0$ respectively.

number of IKS can lead to even more complicated scenarios and will be discussed in the future. A closed loop trajectory in the slice shown in 2b that starts from point $\mathbf{a}(-90, 200)$ and passes through $\mathbf{b}(-150, 200)$, $\mathbf{c}(-150, 375)$, $\mathbf{d}(75, 375)$ and $\mathbf{e}(75, 200)$ is bound to sudden jumps and getting off the expected path no matter which initial IKS is chosen. The two examples discussed in the paper demonstrate the challenges in path planning for a cuspidal robot. These examples are not related to any special poses, the only condition used to demonstrate the issues in path planning is that it travels through multiple connected regions in the workspace. It suffices to say that the cuspidality analysis is essential particularly in the present scenario when designers choose unconventional designs. The issues in the trajectory planning of a cuspidal robot make it necessary that such robots are limited to applications involving a known environment and use of pre-planned trajectories.

VI. CONCLUSIONS AND FUTURE WORK

In this work, an example of a cuspidal commercial robot employed in applications involving human interaction is presented. This robot is close to conventional Puma-type

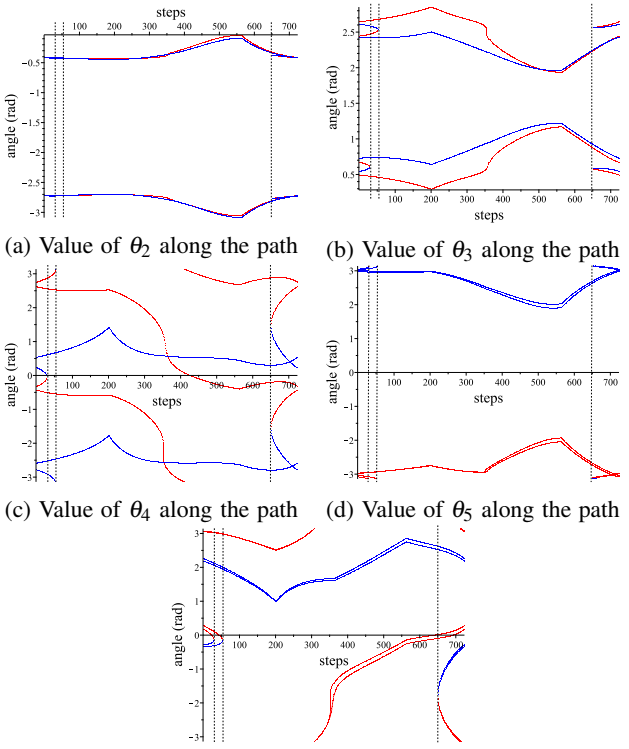

(a) Value of θ_2 along the path (b) Value of θ_3 along the path

(c) Value of θ_4 along the path (d) Value of θ_5 along the path

(e) Value of θ_6 along the path

Fig. 11: Plot for $\theta_{2\ldots6}$ of all solutions at discretized points along the path in fig. 9.

robots but has a wrist offset. The kinematic analysis with the different IKS and the major difference from conventional wrist-partitioned robots has been detailed. The JACO robot was shown to be cuspidal with the help of connectivity analysis of the twelve IKS of the robot. A nonsingular change of solutions for the robot was then presented. The problems in trajectory planning arising from the innate kinematic property of the JACO robot was introduced. The issues related to the initial choice of IKS as well as the repeatability of a given path were detailed with an example trajectory. Many existing industrial robots like FANUC CRX series and Kinova Link 6 are cuspidal robots and thus the risks of deploying cuspidal robots in collaborative environments were also explained. In future, the cuspidality analysis of robots will be conducted considering joint limits and collision constraints. This will help analyzing practically feasible paths and their nature enhancing the trajectory planning of cuspidal robots. A path planning framework for cuspidal robots is also being designed to mitigate the issues presented in this paper.

ACKNOWLEDGMENT

The authors are supported by the joint French and Austrian ECARP project: ANR-19-CE48-0015, FWF I4452-N. The authors also thank Achille Verheyes, Freedom Robotics, for sharing his experience on trajectory planning with cuspidal robots in real world application.

REFERENCES

[1] V. Parenti-Castelli and C. Innocenti, "Position analysis of robot manipulators: Regions and subregions," in *Proceedings of 1988 conference on Advances in Robot Kinematics*, Ljubljana, Sept. 1988, pp. 151–158.

[2] J. W. Burdick, "On the Inverse Kinematics of Redundant Manipulators: Characterization of the Self-Motion Manifolds," in *1989 International Conference on Advanced Robotics*, vol. 4, Ohio, 1989, p. 10.

[3] J. El Omri and P. Wenger, "How to recognize simply a non-singular posture changing 3-dof manipulator," in *Proc. 7th Int. Conf. on Advanced Robotics*, 1995, pp. 215–222.

[4] C. Innocenti and V. Parenti-Castelli, "Singularity-free evolution from one configuration to another in serial and fully-parallel manipulators," *ASME Journal of Mechanical Design*, vol. 120, pp. 73–99, 1998.

[5] P. Wenger and D. Chablat, "A Review of Cuspidal Serial and Parallel Manipulators," *Journal of Mechanisms and Robotics*, vol. 15, no. 4, 11 2022, 040801. [Online]. Available: https://doi.org/10.1115/1.4055677

[6] P. Borrel and A. Liegeois, "A study of multiple manipulator inverse kinematic solutions with applications to trajectory planning and workspace determination," in *Proceedings. 1986 IEEE International Conference on Robotics and Automation*, vol. 3, San Francisco, CA, USA, 1986, pp. 1180–1185.

[7] P. Wenger, "A New General Formalism for the Kinematic Analysis of All Non-redundant Manipulators," in *Proceedings of the 1992 IEEE International Conference on Robotics and Automation*, Nice, France, May 1992, pp. 442–447.

[8] P. Wenger and J. El Omri, "Comments on "A classification of 3R regional manipulator geometries and singularities"," *Mechanism and Machine Theory*, vol. 32, no. 4, pp. 529–532, May 1997.

[9] M. Baili, P. Wenger, and D. Chablat, "A classification of 3R orthogonal manipulators by the topology of their workspace," in *IEEE International Conference on Robotics and Automation, 2004. Proceedings. ICRA '04. 2004*. New Orleans, LA, USA: IEEE, 2004, pp. 1933–1938 Vol.2.

[10] P. Wenger, "Uniqueness Domains and Regions of Feasible Paths for Cuspidal Manipulators," *IEEE Transactions on Robotics*, vol. 20, no. 4, pp. 745–750, Aug. 2004.

[11] P. Wenger, D. Chablat, and M. Baili, "A DH-parameter based condition for 3R orthogonal manipulators to have 4 distinct inverse kinematic solutions," *ASME Journal of Mechanical Design*, vol. 127, pp. 150–155, 2005.

[12] P. Wenger, "Cuspidal and noncuspidal robot manipulators," *Robotica*, vol. 25, no. 6, pp. 677–689, Nov. 2007.

[13] D. H. Salunkhe, C. Spartalis, J. Capco, D. Chablat, and P. Wenger, "Necessary and sufficient condition for a generic 3r serial manipulator to be cuspidal," *Mechanism and Machine Theory*, vol. 171, p. 104729, 2022.

[14] D. Chablat, R. Prébet, M. Safey El Din, D. H. Salunkhe, and P. Wenger, "Deciding Cuspidality of Manipulators through Computer Algebra and Algorithms in Real Algebraic Geometry," in *2022 International Symposium on Symbolic and Algebraic Computation*, Lille, France, July 2022.

[15] A. Verheye. (2021) Why hasn't anyone heard of cuspidal robots?, http://achille0.medium.com/why-has-no-one-heard-of-cuspidal-robots-fa2fa60ffe9b. [Online]. Available: http://achille0.medium.com/why-has-no-one-heard-of-cuspidal-robots-fa2fa60ffe9b

[16] J. Capco, M. Safey El Din, and J. Schicho, "Robots, computer algebra and eight connected components," in *ISSAC '20: International Symposium on Symbolic and Algebraic Computation*, ser. ISSAC'20: Proceedings of the 45th International Symposium on Symbolic and Algebraic Computation. Kalamata / Virtual, Greece: ACM, July 2020, pp. 62–69.

[17] D. L. Pieper, "The Kinematics of Manipulators Under Computer Control," Ph.D. dissertation, Stanford University, USA, Oct. 1968.

[18] [Online]. Available: http://kinovarobotics.com

[19] P. Wenger and J. El Omri, "Changing posture for cuspidal robot manipulators," in *Proceedings of IEEE International Conference on Robotics and Automation*, vol. 4. Minneapolis, MN, USA: IEEE, 1996, pp. 3173–3178.

[20] M. Raghavan and B. Roth, "Inverse Kinematics of the General 6R Manipulator and Related Linkages," *ASME Journal of Mechanical Design*, vol. 115, no. 3, pp. 502–508, 09 1993.

[21] M. L. Husty, M. Pfurner, and H.-P. Schröcker, "A new and efficient algorithm for the inverse kinematics of a general serial 6r manipulator," *Mechanism and Machine Theory*, vol. 42, no. 1, pp. 66–81, 2007.

[22] C. Trinh, D. Zlatanov, M. Zoppi, and R. Molfino, "A Geometrical Approach to the Inverse Kinematics of 6R Serial Robots With Offset Wrists," ser. International Design Engineering Technical Conferences and Computers and Information in Engineering Conference, vol. Volume 5C: 39th Mechanisms and Robotics Conference, 08 2015.

[23] C. Gosselin and H. Liu, "Polynomial Inverse Kinematic Solution of the Jaco Robot," ser. International Design Engineering Technical Conferences and Computers and Information in Engineering Conference, vol. Volume 5B: 38th Mechanisms and Robotics Conference, 08 2014.

[24] F. Rouillier, "Solving zero-dimensional systems through the rational univariate representation," *Journal of Applicable Algebra in Engineering, Communication and Computing*, vol. 9, pp. 433–461, 05 1999.

[25] J. A. Nelder and R. Mead, "A Simplex Method for Function Minimization," *The Computer Journal*, vol. 7, no. 4, pp. 308–313, 01 1965.

[26] D. Kohli and J. Spanos, "Workspace Analysis of Mechanical Manipulators Using Polynomial Discriminants," *Journal of Mechanisms, Transmissions, and Automation in Design*, vol. 107, no. 2, pp. 209–215, June 1985.

[27] M. Husty, E. Ottaviano, and M. Ceccarelli, *A Geometrical Characterization of Workspace Singularities in 3R Manipulators*. Dordrecht: Springer Netherlands, 2008, pp. 411–418.